AD-A050 464 SRI INTERNATIONAL MENLO PARK CA F/G 20/6
TECHNIQUES FOR THE MICROFABRICATION OF INTEGRATED OPTICAL WAVEG--ETC(U)
JAN 78 E R WESTERBERG, I BRODIE N00173-76-C-0174

UNCLASSIFIED NL

| OF |
AD
A050464

END
DATE FILMED
3-78
DDC

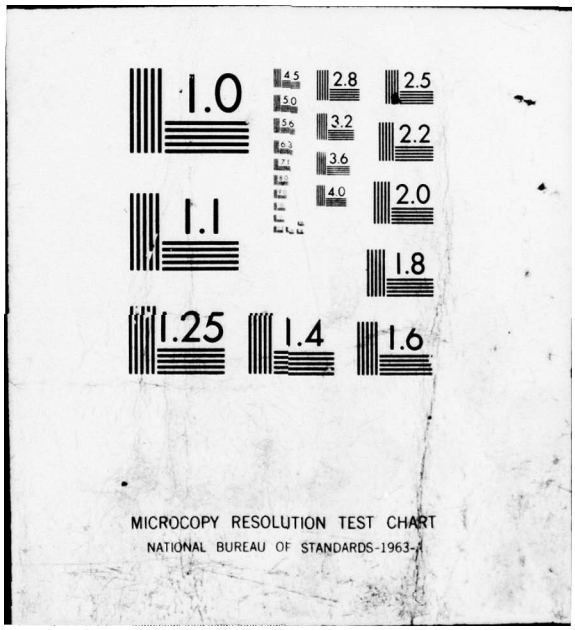
1.0
1.1
1.25
1.4
1.6
1.8
2.0
2.2
2.5
2.8
3.2
3.6
4.0
4.5
5.0
5.6
6.3
MICROCOPY RESOLUTION TEST CHART
NATIONAL BUREAU OF STANDARDS-1963-A

SRI International

TECHNIQUES FOR THE MICROFABRICATION OF INTEGRATED OPTICAL WAVEGUIDE COUPLERS

Final Technical Report

January 1978

By: Eugene R. Westerberg
Ivor Brodie

Prepared for:

Optical Physics Research Group
Naval Research Laboratory
Washington, DC 20375

Contract N00173-76-C-0174

SRI Project 5303

SRI International

333 Ravenswood Ave. • Menlo Park, California 94025
(415) 326-6200 • Cable: STANRES, Menlo Park • TWX: 910-373-1246

UNCLASSIFIED

SECURITY CLASSIFICATION OF THIS PAGE (When Data Entered)

REPORT DOCUMENTATION PAGE

READ INSTRUCTIONS BEFORE COMPLETING FORM

1. REPORT NUMBER

2. GOVT ACCESSION NO.

3. RECIPIENT'S CATALOG NUMBER

4. TITLE (and Subtitle)

TECHNIQUES FOR THE MICROFABRICATION OF INTEGRATED OPTICAL WAVEGUIDE COUPLERS

5. TYPE OF REPORT & PERIOD COVERED

Final Report, covering the period 14 Apr 76 – 13 Jan 77

6. PERFORMING ORG. REPORT NUMBER

SRI Project 5303

7. AUTHOR(s)

Eugene R. Westerberg
Ivor Brodie

8. CONTRACT OR GRANT NUMBER(s)

N00173-76-C-0174

9. PERFORMING ORGANIZATION NAME AND ADDRESS

SRI International
333 Ravenswood Avenue
Menlo Park, California 94025

10. PROGRAM ELEMENT, PROJECT, TASK AREA & WORK UNIT NUMBERS

11. CONTROLLING OFFICE NAME AND ADDRESS

Optical Physics Research Group
Naval Research Laboratory
Washington, DC 20375

12. REPORT DATE

Jan 78

13. NUMBER OF PAGES

35

14. MONITORING AGENCY NAME & ADDRESS (if different from Controlling Office)

15. SECURITY CLASS (of this report)

Unclassified

15a. DECLASSIFICATION/DOWNGRADING SCHEDULE

N/A

16. DISTRIBUTION STATEMENT (of this Report)

DISTRIBUTION STATEMENT A
Approved for public release;
Distribution Unlimited

17. DISTRIBUTION STATEMENT (of the abstract entered in Block 20, if different from Report)

18. SUPPLEMENTARY NOTES

19. KEY WORDS (Continue on reverse side if necessary and identify by block number)

20. ABSTRACT (Continue on reverse side if necessary and identify by block number)

This report covers the development of techniques for the microfabrication of integrated optical waveguide couplers. In particular an Electron Projection Exposure System (EPES), that uses a large-area electron beam to image an object transmission mask with a size reduction of a factor of twenty, was studied in detail.

Techniques for fabricating transmission masks for EPES were successfully developed. Additional features were added to the original SRI electron optical column to make it applicable for IO device lithography, including mask alignment fixtures, a sample stage with external positioning drivers with a precision of 1000 Å, and an electron projection lens with a resolution of 0.5 microns and an edge sharpness of 500 Å. However, the problem of uniformly illuminating the object transmission mask with electrons proved to be extremely difficult to resolve, and

DD FORM 1 JAN 73 1473 EDITION OF 1 NOV 65 IS OBSOLETE

UNCLASSIFIED

SECURITY CLASSIFICATION OF THIS PAGE (When Data Entered)

410 281

20. ABSTRACT (Continued)

for this reason the fabrication of a complete optical waveguide coupler using the EPES technique was not attempted.

Techniques for indiffusing titanium strips on a lithium niobate substrate to obtain planar guides were developed, and attempts were made to produce devices using optical contact lithography and a high resolution mask supplied from an external vendor via NRL.

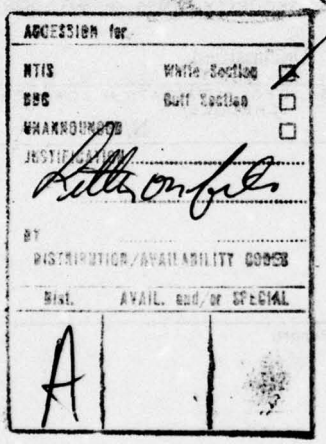

CONTENTS

ILLUSTRATIONS

I INTRODUCTION

This report describes work carried on at SRI in the microfabrication of structures that are useful in the field of integrated optics (IO). IO devices utilize solid-state methods to manipulate light signals by using such components as sources, detectors, modulators, and couplers, all fabricated on suitable substrates to produce systems that are much smaller than conventional optical systems. Because of the high frequency of the entrained electromagnetic waves, these components have the advantage of operating with very large bandwidths. Their small size makes IO systems much less susceptible to temperature changes, mechanical vibrations, and electromagnetic fluctuations than systems using conventional optics. Significant advantages of these systems for military application include secure communication (freedom from signal leakage), elimination of extraneous noise pickup due to grounding problems, and low susceptibility of electromagnetic interference. The major objective of the work described in this report was to fabricate devices which could be used to test the principles of operation of a novel integrated optical waveguide coupler designed at the Naval Research Laboratory.

The production of IO structures requires advanced technology in both lithographic (pattern-production) and thin-film techniques. In particular, the requirements of the lithographic technology are stringent. Waveguides and coupling structures with guiding dimensions of only a few micrometers are required, and total device dimensions (e.g., coupler lengths in IO devices) of longer than 1 mm are necessary. Furthermore, the edge acuities of the light-guiding components must be better than 1000 Å, so that light is not scattered out of the guides to create signal-to-noise ratio and crosstalk problems. Available lithographic techniques for producing IO structures of this type fall into three categories, depending on the exposure means: light, x-ray, or electron.

Photolithography is the oldest of the techniques. Here, either the desired pattern is optically projected onto a light-sensitive resist material, or a mask is placed in direct contact with the photoresist-coated sample to produce a one-to-one copy. The photoprojection technique allows the pattern of the master transmission mask to be much

larger than the final pattern, thus greatly simplifying mask production. The optical projection system then demagnifies the pattern of the transmission mask to produce a latent image in the photoresist. Because of the basic diffraction limitation imposed by the wavelength of light and the projection optics, the resolution with present-day optical projection systems is approximately 1 to 2 μm.[1]* This resolution appears to be insufficient for the production of good 1-μm-wide optical waveguide structures.

Contact photolithography has recently made a significant advance with the introduction of the flexible mask.[2] This technique employs a very thin glass mask which is placed in a vacuum frame above a photoresist-coated sample. When the frame has been evacuated, the flexible mask is forced into intimate contact with the sample surface. With this technique, resolutions of somewhat below a micron can be obtained. However, several problems arise in applying the technique to the microfabrication of integrated optical structures. Unlike the optical projection system, this technique requires the mask pattern to be the same size as the final image, and so the mask needs to be fabricated with submicron detail if the image is to contain submicron detail. Producing such a mask requires other types of lithography with higher resolution, e.g., electron beam lithography. The flexible-mask contact exposure process also suffers from a loss of edge definition because of diffraction in resolution is the capability of resolving two distinct points--separated by the minimum distance. A lack of edge definition (caused by the diffraction effects in a photoresist layer of finite thickness) can lead to wavy edges on waveguides. This edge imperfection produces extra scattering and increases loss from the waveguides. However, during the course of the work reported here, NRL was able to obtain from a commercial supplier (Qualitron) an optical mask with sufficient resolution to test out the principles of their integrated optical waveguide coupler.

---

*References are listed at the end of the report.

X-ray lithography uses soft x-rays to expose a suitable x-ray-sensitive resist material through a shadow mask.[3] The wavelength of the x-rays is typically 1,000 times shorter than that of visible light, and thus the resolution and the edge definition of this technique are superior to those achieved by photolithography. However, as with contact photolithography, the x-ray technique requires a mask with the same resolution as the final image.

Electron beam lithography can be classified into two categories: scanning and projection. The scanning technique uses a fine focused beam of electrons; the pattern is created in an electron-sensitive resist by appropriately deflecting this beam with a set of magnetic deflection coils. The effective wavelength of the electrons is below an angstrom, and diffraction is no problem with this technique. The resolution is generally limited by the thickness of the electron-sensitive resist, and resolutions on the order of 0.1 μm have been demonstrated. The equipment for scanning electron beam lithography is fairly complex and costly. A fabrication facility needs a scanning electron microscope (SEM) that has been modified for lithographic applications, a computer to produce the scan data, and an interfacing system to provide transfer of information between the SEM and the computer.

Two types of projection systems are used in electron lithography. In the electron image projection system (ELIPS) the pattern to be transferred is reproduced on a photocathode.[4] When this cathode is illuminated by strong ultraviolet radiation, photoelectrons are emitted in the pattern, and a uniform magnetic field focuses these electrons onto the substrate surface. Large areas of exposure, high resolution, and good edge definition are possible with this technique. However, the electron optics of the process provide unity magnification, and hence pattern demagnification is not possible.

A second type of electron projection system is the analog of the optical projection system described above. It uses a transmission mask (a mask with cutout areas transparent to electrons) as an object, demagnifies this mask with an electron optical system, and projects the image onto an electron-sensitive resist surface. This system has the advantage

of high resolution and good edge acuity because of the short wavelength of the electrons. It provides a projection demagnification in the range of 20 to 200X, so the transmission masks can be produced on a large scale with standard photolithographic techniques and then be reduced to the required scale with the projection system. In projection systems all portions of the image are exposed simultaneously, whereas in scanning systems the image is built up serially, one image point at a time. Consequently, the exposure times of projection systems are substantially less than the times for comparable patterns produced with scanning systems. Since an electron projection system uses a transmission mask as an object, special design attention must be given to the pattern etched into the mask, to ensure that all portions of the pattern are properly supported. For the centers of designs that would not normally be supported (e.g., the center of the letter "O"), bridge supports that are small enough so that they cannot be resolved in the image must be built into the mask.

II THE SRI ELECTRON PROJECTION EXPOSURE SYSTEM (EPES)

The SRI EPES is an outgrowth of a one-dimensional projection system (the slit-lens exposure system) developed under ARPA Contract DAHC15-72-C-0265. The slit-lens exposure system uses a transmission mask in which a pattern of holes is transformed into a pattern of straight lines by using a one-dimensional aperture lens (slit). Lines produced with the slit lens have high edge definition and widths as small as 0.34 μm, with interline spacings of 0.68 μm. This particular exposure system has proved useful in the fabrication of such structures as surface acoustic wave transducers, Barker-coded devices, and integrated optical waveguide masks.

The EPES uses a modified projection aperture lens to achieve two-dimensional imaging, so that a faithful image of a transmission mask can be projected onto a resist-coated substrate surface. Figure 1 shows the basic components of SRI's EPES. Electrons from a simple gun and condensing lens structure, here represented by a filament, illuminate a

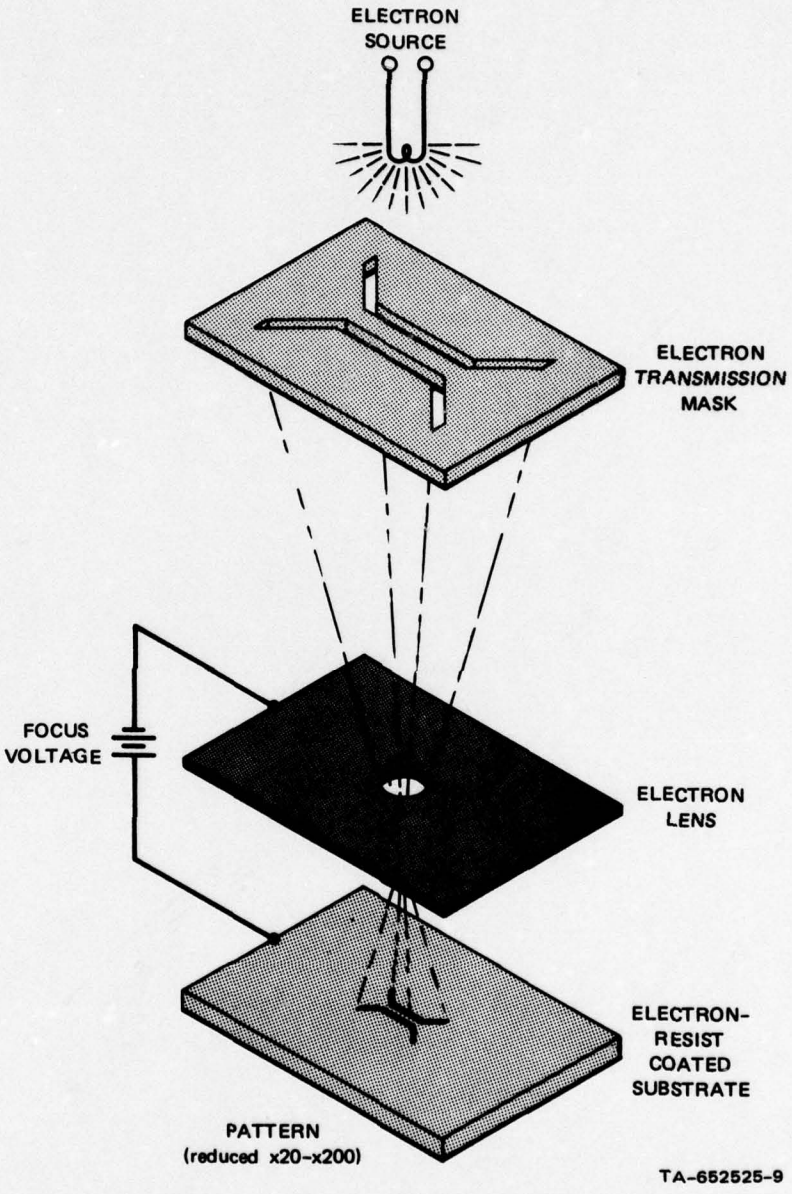

FIGURE 1 ELECTRON BEAM PROJECTION LITHOGRAPHY

transmission mask. In this schematic diagram, a typical 3-dB integrated optical coupler illustrates a possible mask configuration. The transmitted electrons converge on the objective lens and an aperture lens and are focused onto the electron resist-coated substrate. Figure 2 depicts the focusing action of a simple aperture lens. The lens here is merely a round hole in a conducting plane. If the appropriate voltage is applied between this conducting lens plane and the conducting surface of the sample, the electrons will be brought to a focus at the sample surface. A higher-resolution image can be obtained by using a second aperture as a beam limiter in the field-free, object side of the lens. This aperture, with a diameter of 25 to 50% of the lens diameter, eliminates the highly aberrated electron rays that would be produced near the rim of the lens hole.

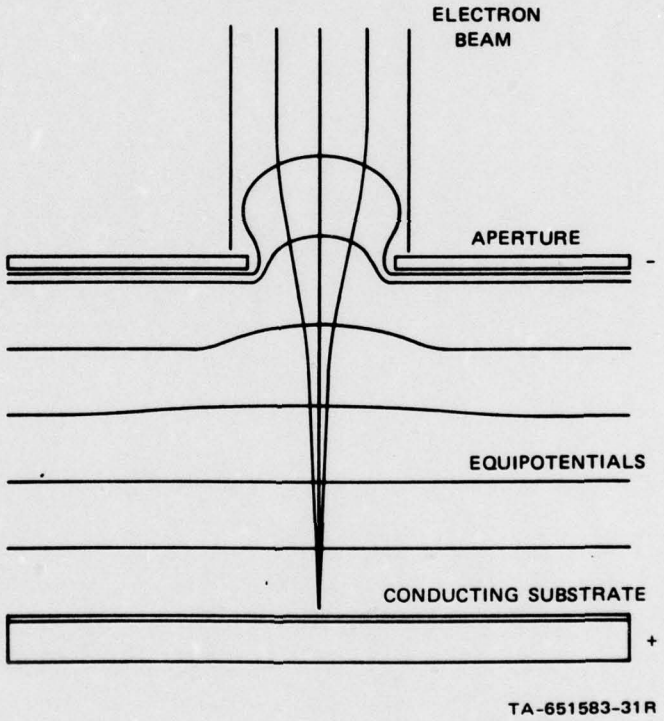

FIGURE 2 APERTURE LENS ACTION

This projection aperture lens has a number of advantages. First, it is a very simple electrostatic lens. Other types of lenses require an exact registration of a number of optical elements, but this lens requires virtually no alignment to obtain high resolution. A second feature of the aperture lens lies in its self-focusing property. First-order theory shows that, if a focusing potential of 8Φ (where Φ is the energy of the electrons as they traverse the transmission mask) is applied between the lens plane and the sample, highly demagnified images will always be in focus at the substrate plane, regardless of aperture-to-substrate spacing--i.e., the EPES has a large depth of focus. This feature makes the lens system exceptionally tolerant to substrate unevenness, which often limits the resolution of other projection and contact exposure systems. The demagnification of the EPES can be varied over a wide range by merely changing the lens-to-substrate distances. Thus, pattern production is greatly facilitated, since small magnification changes can be effected by altering the lens-substrate spacing without refocusing.

Aperture lenses possess still another interesting feature. The ultimate resolution of an electron-optical lens system is mainly determined by the spherical aberration of the system. The point-source electrons that pass near the periphery of the lens are strongly deflected to cross the axis nearer the lens than the electrons that pass through the center of the lens. This defect is called spherical aberration, and the increase in spot size is given by:

$$\delta = C_3\gamma^3 + C_5\gamma^5 + \ldots \quad ,$$

where γ is the semiangle of lens illumination, and C_5^3 and C_5 are the third- and fifth-order spherical aberration coefficients, respectively. Ray tracing on the SRI computer has shown that the coefficients C_3 and C_5 have opposite signs for aperture lenses. Thus, when the angle γ gets large enough, the spherical aberration is partially cancelled out. This enables such a lens to be used at wider apertures than is normally possible.

The SRI EPES was constructed in a modular fashion, as shown in Figure 3. The two main electron optical elements, i.e., the illumination system and the projection aperture lens, are housed in opposite ends of a fully demountable, self-aligning vacuum column and shield. Electrons from the cathode at the bottom of the column are formed into a wide beam by a grid electrode and an anode. This beam is directed through an electron lens which acts as a condensing lens. The strength of the lens is adjusted so that an image of the cathode is formed at the plane of the aperture lens. This condition ensures that as large an area as possible on the transmission mask is illuminated in the final image. The transmission mask with the desired pattern is placed as close as possible to the final electrode of the condensing lens.

Two sets of orthogonal electrostatic deflectors are used to adjust the positions of the converging beam so that it is positioned on the aperture of the projection lens. The projection lens assembly consists of two components, the aperture lens proper and a beam limiting aperture plate which serves to keep the beam confined to the high resolution central region of the aperture lens. The final part of the system is the sample holder. Magnification in the system is established by the spacing between the aperture lens and the sample holder.

In more detail the EPES can be described as follows.

Gun: The gun shown in Figure 4 has a cathode of the Phillips matrix type with a diameter of 0.3 inch. The system needs a large cathode to provide a uniform illumination pattern and compensate somewhat for the spherical aberration of the condensing lens. The cathode is activated in the system by heating it to 1150°C for 5 minutes, the temperature being measured directly from the emitting surface with a radiation pyrometer. In normal operation the temperature is reduced to 1050°C. Since the entire system must be brought up to atmospheric pressure between exposures, to enable the sample to be removed, the column is backfilled with dry nitrogen before opening, to extend the life of the cathode. Typical cathodes can withstand 40 to 50 cycles to atmospheric pressure before their emission patterns grow so patchy that they cannot provide the required uniformity.

FIGURE 3 ELECTRON PROJECTION EXPOSURE SYSTEM

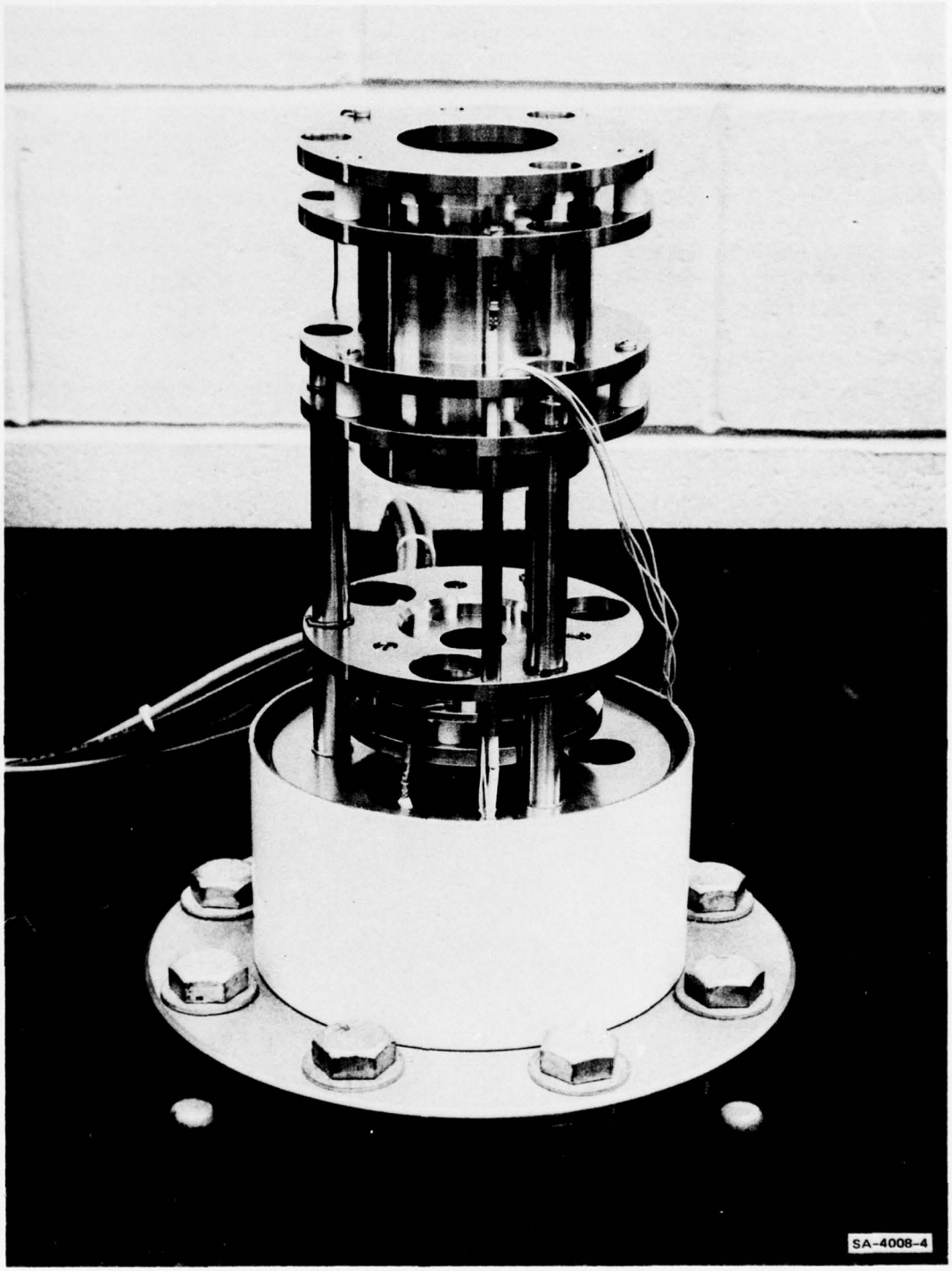

FIGURE 4 ELECTRON GUN

The grid electrode and anode are constructed of 316 stainless steel; each has a central 0.5-inch-diameter hole; and the interelectrode spacing is 0.5 inch. The anode is operated at ground potential, while the grid is held near the cathode potential, -500 V. The best pattern coverage seems to be obtained with the grid run slightly positive with respect to the cathode (0 to +15 V).

Condenser Lens: The top of the gun shown in Figure 4 is the condensing lens structure. The structure is built in an erector-set fashion on a set of three supporting rods. This configuration makes it easy to modify the illumination system. Several lens configurations were assembled and tested. Performance depends mainly on the spherical aberration of the lens, which shows up as an unevenly illuminated image on the sample surface. Since the transmission mask is positioned very close to the condenser lens, portions of the pattern near the periphery are illuminated by electrons that are considerably off axis in the condenser lens. The spherical aberration causes these marginal electron rays to be focused closer to the lens than the paraxial rays, i.e., those through the lens center. Thus, if the paraxial rays are focused on the projection lens, the overfocus of the marginal rays prevents them from contributing to the image, and the spherical aberration establishes the maximum pattern diameter that can be produced.

The best lens configuration that we have determined for the condenser is the einzel lens, a three-electrode lens in which the outer two electrodes are run at ground potential and the inner electrode near cathode potential, i.e., typically 50 to 100 V positive with respect to the cathode. The lens plates for this configuration have a relatively large bore (2.00-inch diameter), and the interelectrode spacing is 1.00 inch. An aperture in front of the lens limits the entering rays to a bundle of about 1-inch diameter. The focal length of the lens is approximately 7 inches. Third-order spherical aberration limits the effective area of illumination to 0.4 inch at the transmission mask plane.

Substantial improvements in illumination areas was found to be very difficult to realize by further improvements in condenser lens design or spherical aberration reductions. Since the aberration diameter at the beam-limiting aperture plane is proportional to $C_s d^3$, where C_s is the spherical aberration coefficient and d is the beam diameter at the mask, a decrease in C_s of almost 16 times must be achieved to effect an increase of d from 0.4 inch to 1.0 inch. This problem was examined theoretically, and no lens configuration was found that would give such a large spherical aberration reduction.

We used another approach to increase the effective area of illumination. If an alternating potential is applied to the center electrode of the condensing lens, the focus of the lens is continuously altered so that some of the marginal rays of the condenser lens can be brought to focus through the projection lens. We built a focus control system for the condenser that allows various ac waveforms to be superimposed on the dc focus potential. Sine, triangle, square, and ramp waveforms were tested for the best illumination characteristics. Sine waves proved to be the most useful and we were able to extend the illumination area diameter from 0.4 inch to 0.55 inch by applying a sine wave of 15 V_{rms} to the center electrode (dc potential ~ -450 V). However, this method is not perfect because the marginal rays pass through the beam-limiting aperture only periodically, whereas the paraxial rays are focused virtually continuously, resulting in a pattern with a bright central region; and we were unable to overcome this problem.

Transmission Mask Positioner: With electron projection, each transmission mask pattern is reduced to cover an area with side lengths of about 0.65 mm, but to fashion entire IO devices it is necessary to cover a length of 2 mm or more. Since this cannot be accomplished in a single exposure with out system, we built a transmission mask positioner into the EPES. This positioner enables us to change patterns without breaking vacuum; when it is used in conjunction with an accurately positionable sample stage, we can register a number of patterns on the substrate and thus form an extended pattern by sequential exposure.

The mask positioner is shown in Figure 5. It has provisions for eight independently alignable masks. Each mask is 0.75 inch square. The positioner was built to fit our 6-inch-diameter column as a modular unit. However, to accommodate eight masks, the diameter of the unit was increased to 14 inches. All the masks are mounted on a large rotary stage that can be turned from outside the exposure system through a vacuum seal, and the alignment of the mask pattern is ensured by use of a hardened tapered pin as an alignment dowell. This pin was hand-lapped to give positional repeatability of better than 2 μm. The entire rotary positioner can be easily removed from the projection system and placed under a toolmaker's microscope where each mask can be aligned independently to an accuracy of 0.0001 inch. After electron optical 20× reduction, the error is of the order of 1000 Å and should be tolerable for IO devices.

Deflectors: As can be seen in Figure 6 the beam-positioning deflectors are simple electrostatic plates placed immediately after the mask holder. Because of the small deflection angle, generally less than 10 mrad, there is no need to optimize their design for low aberration. Deflection voltages are applied differentially, and for alignment dc voltages of about ±20 V are required for the 300-eV beam.

Projection Lens: The heart of the EPES is the aperture lens (Figure 7) that serves to demagnify the pattern on the transmission mask. It is a simply constructed lens consisting of two plates, a beam-limiting aperture plate, and a plate with a somewhat larger diameter hole that functions as the lens proper.

We made theoretical study of aperture lenses to determine the resolution capabilities of various lens designs. Figure 8 summarizes the results of this work. This figure depicts the normalized radius of the circle of least confusion as a function of the normalized aperture radius; i.e., it shows how resolution is limited by the third-order spherical aberration as the aperture of the lens is increased. Here, δ_{CLC} is the radius of the disc of least confusion; R is the radius of the projection

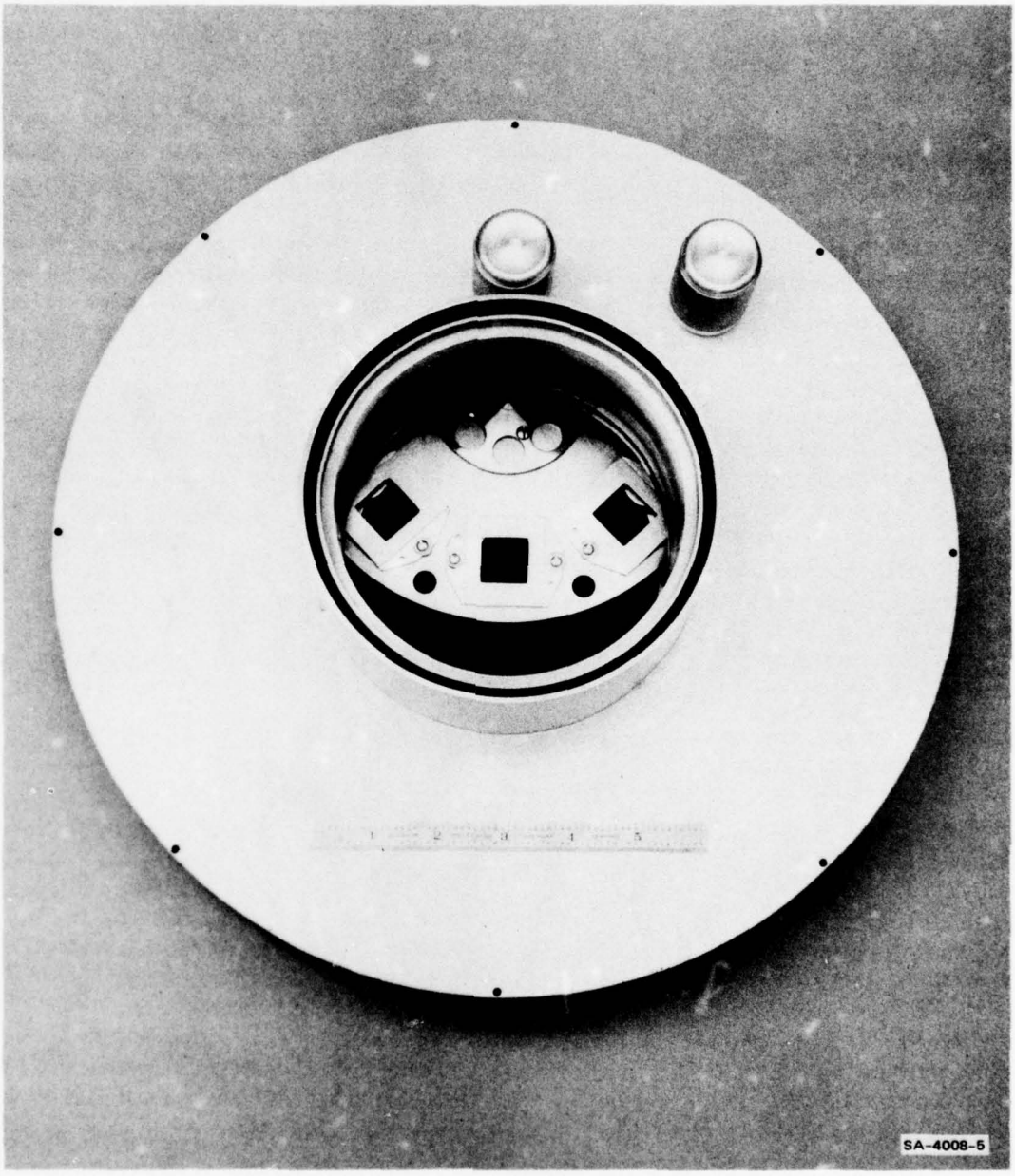

FIGURE 5 TRANSMISSION MASK POSITIONER

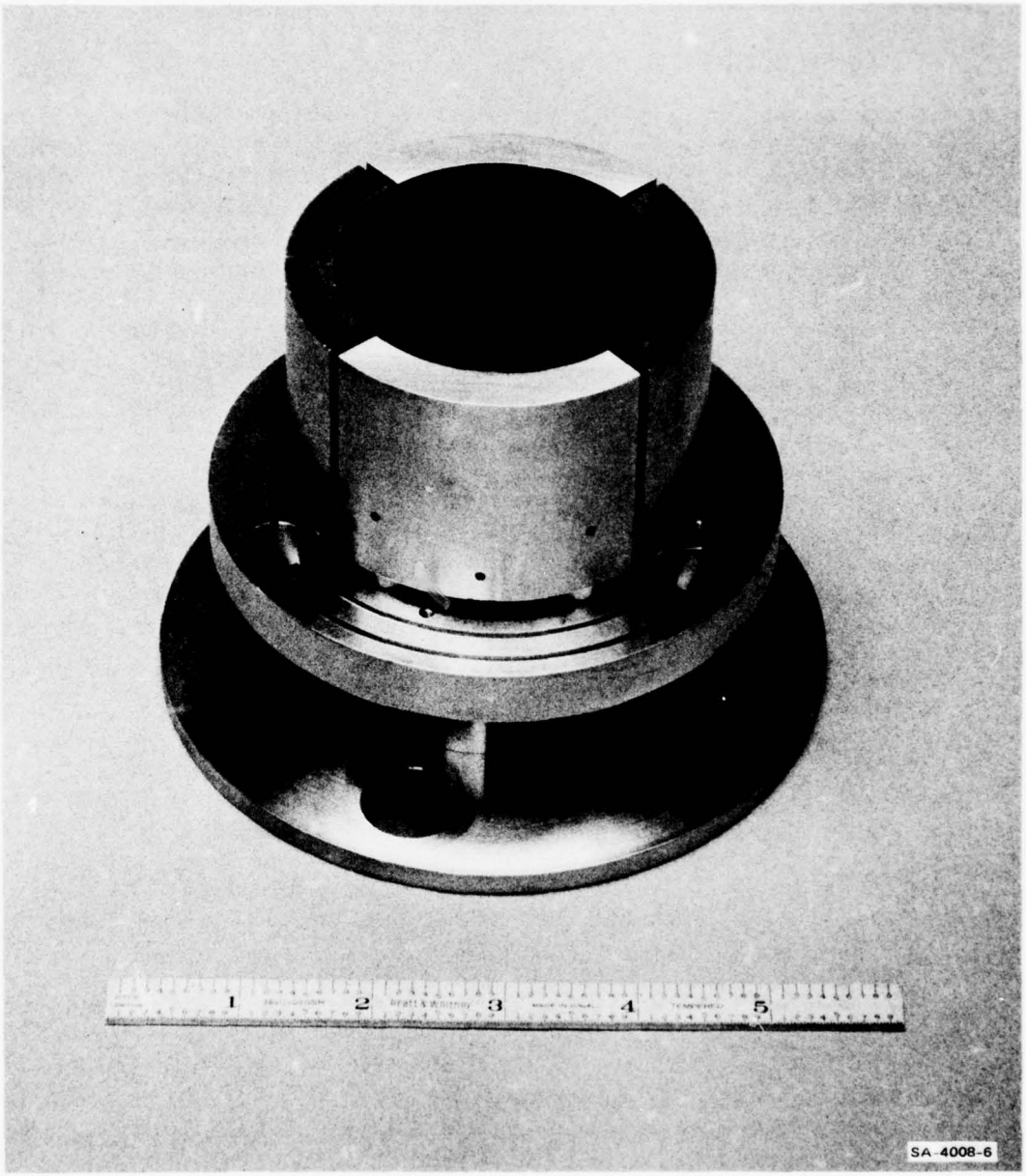

FIGURE 6 DEFLECTORS

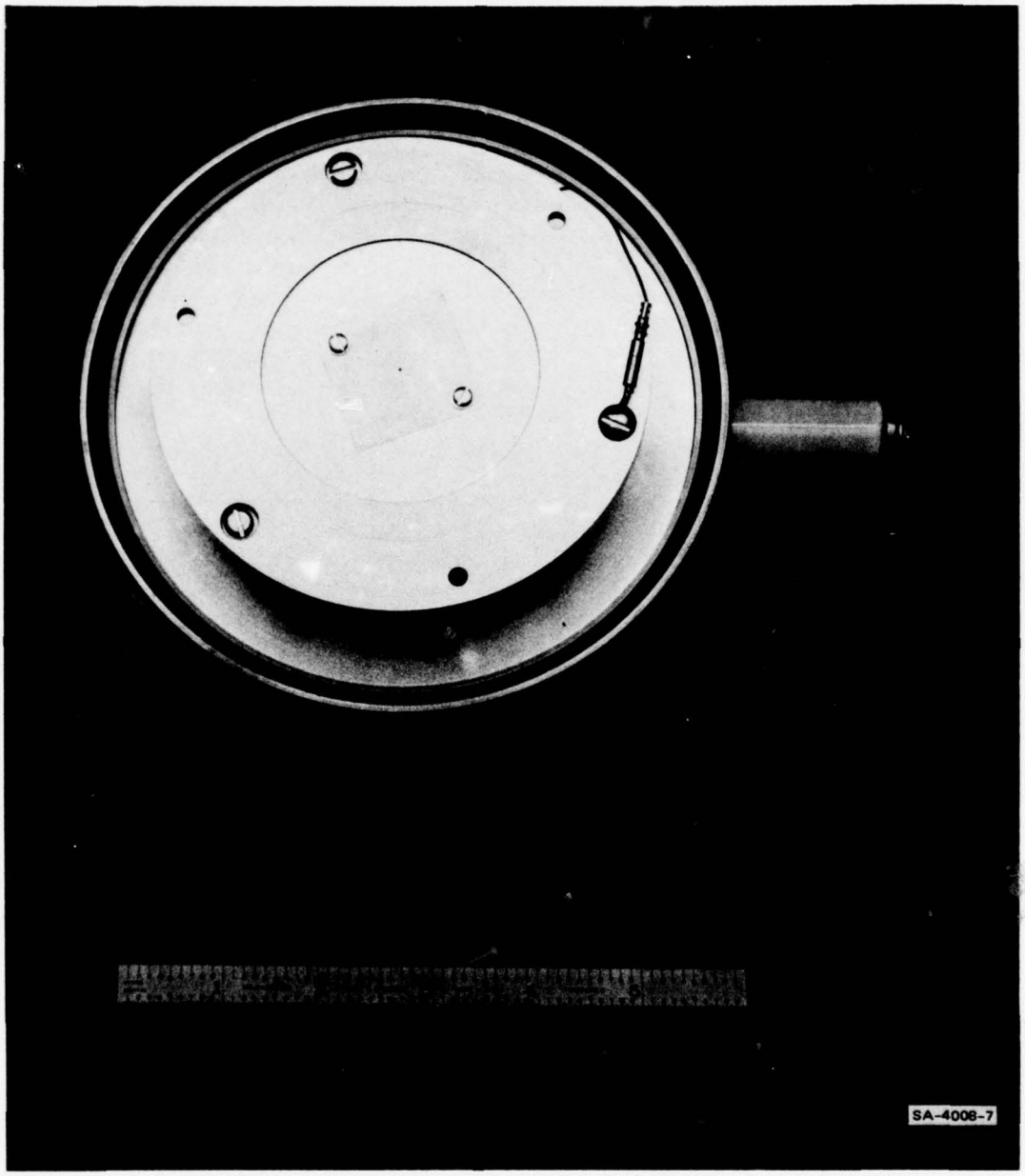

FIGURE 7 PROJECTION LENS AND HOLDER

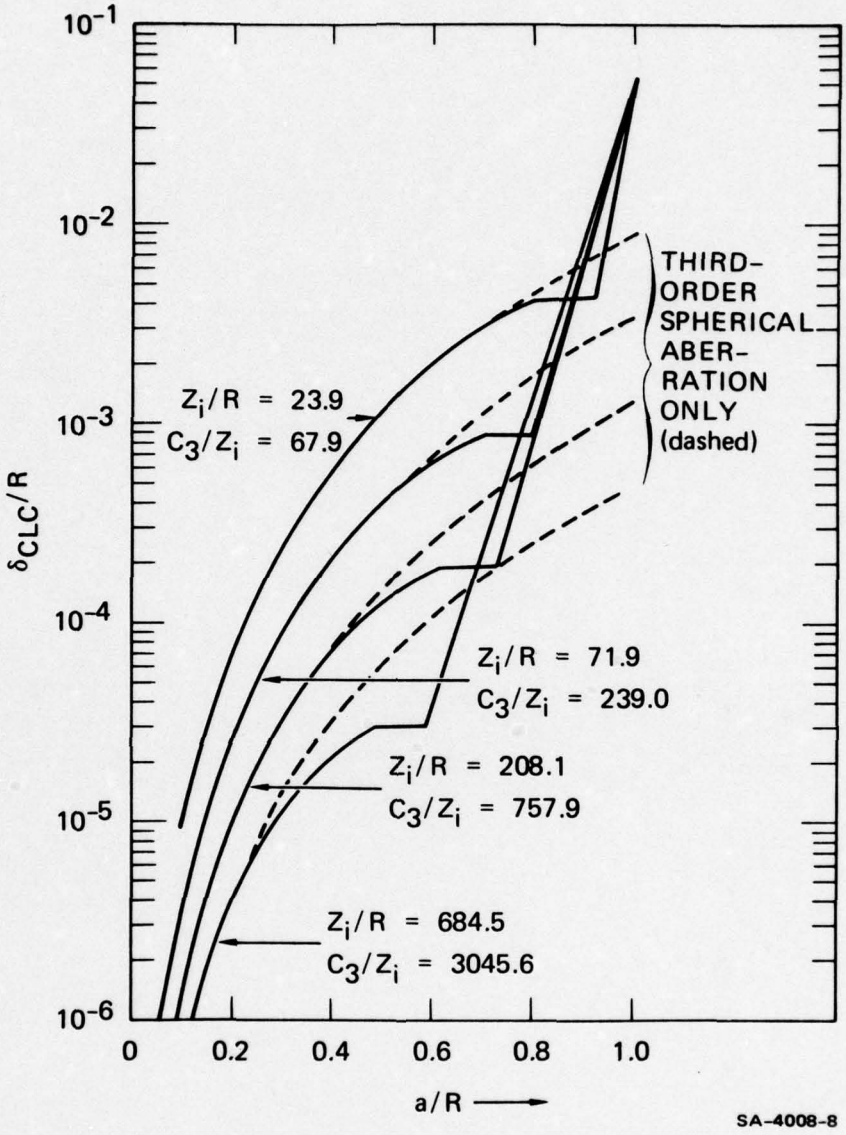

FIGURE 8 APERTURE LENS SPHERICAL ABERRATION

lens; a is the radius of the beam-limiting aperture; Z_i is the lens-to-sample spacing; and C_3 is the third-order spherical aberration coefficient. It is interesting to note that the curves tend to follow the shapes predicted for third-order spherical aberration up to a definite point, after which higher orders (fifth, predominantly) take over, and the curves actually have less total aberration than third-order theory alone would predict. In fact, each curve reaches a plateau during which there is no increase in the circle of least confusion until suddenly, at nearly full aperture, the curves start to increase in an exponential manner. The fact that the aperture lens possesses a negative fifth-order spherical aberration coefficient should make it a very useful imaging lens since normally the higher-order coefficients add more aberration rather than partially correct lower orders.

Our first projection lens consisted of a beam-limiting aperture plate 0.003-inch thick with a 0.005-inch-diameter hole and a lens plate 0.005 inch thick with a 0.010-inch-diameter hole. Separation was 0.030 inch, and the holes were aligned on a mutual axis by adjustment under a 100X toolmaker's microscope. The lens-sample spacing was 0.360 inch. The Zi/R ratio was ~ 72.0; i.e., the second curve from the top of Figure 8. At a/R = 0.5, $\delta_{CLC}/R \cong 4 \times 10^{-4}$, or the resolution should be about 500 Å ($2\ \delta_{CLC}$).

In an effort to partially overcome the effects of the spherical aberration of the condenser lens, we experimented with several other lens combinations. With a larger beam-limiting aperture, it would be expected that more of the spherically aberrated marginal rays would be imaged on the sample, and hence the effective area of illumination would be increased. We used a larger-diameter projection lens (0.020-inch diameter) and beam-limiting apertures of 0.010 inch diameter and 0.016 inch diameter. Theoretical resolutions with a Z_i = 0.500 inch are 3000 Å for the 0.016-inch diameter aperture. Resolution tests made on PMM resist showed a resolution of about 5000 Å for both lenses. The measurements show reasonable agreement with the theory. The first lens may not have performed as well as predicted because of several factors. Astigmatism is not taken into account in the calculations, and a small misalignment

in the lens axes might have increases its contribution. The resist had a thickness of about 2000 Å; within this thickness there will be some resolution degradation because of extra scatter. A significant increase in the area of uniform illumination occurred when the two lenses were used. In the case of the 0.010-inch-diameter aperture this area increased from 0.55-inch diameter (with ac on the central condenser lens electrode) to 0.60 inch, and with the 0.016-inch-diameter aperture the area diameter increased to 0.75 inch, but this was still insufficient to illuminate the entire transmission mask with the necessary uniformity.

Sample Holder: The sample holder was designed for use in conjunction with the rotary mask holder to produce extended coupler patterns. By rotating a new mask into the electron beam and precisely moving the sample in one direction, a series of pattern images can be placed on the sample, each aligned with the previous pattern to make an entire coupler. The stage for the sample holder is shown in Figure 9. Basically, it is a modified translation stage manufactured by Aerotech, Inc. (Allison Park, PA). It was reworked and lubricated to function within a vacuum system at pressures as low as 5×10^{-7} torr. It uses a crossed-roller principle for lateral stability and has a precise linear motion virtually free of backlash and extraneous sideways motion. Positional accuracies of 1 millionth of an inch (250 Å) are claimed to be possible with this stage, and it will traverse distances of up to 2 inches. A laser-controlled interferometric system is used to measure the position of the stage. This system is manufactured by Holograph, Inc. (San Carlos, CA). The stage (within the vacuum system) is connected directly to the interferometer via a rod that passes through an o-ring seal in the vacuum wall. The interferometric system incorporates a precision glass scale ruled with a pattern of interfering light fringes. The position of this glass scale is monitored by counting interference fringes as the scale is moved. Air bearings are used to reduce the sliding friction. The accuracy of the Holograph stage is about an eighth of a fringe of red light (better than 1000 Å).

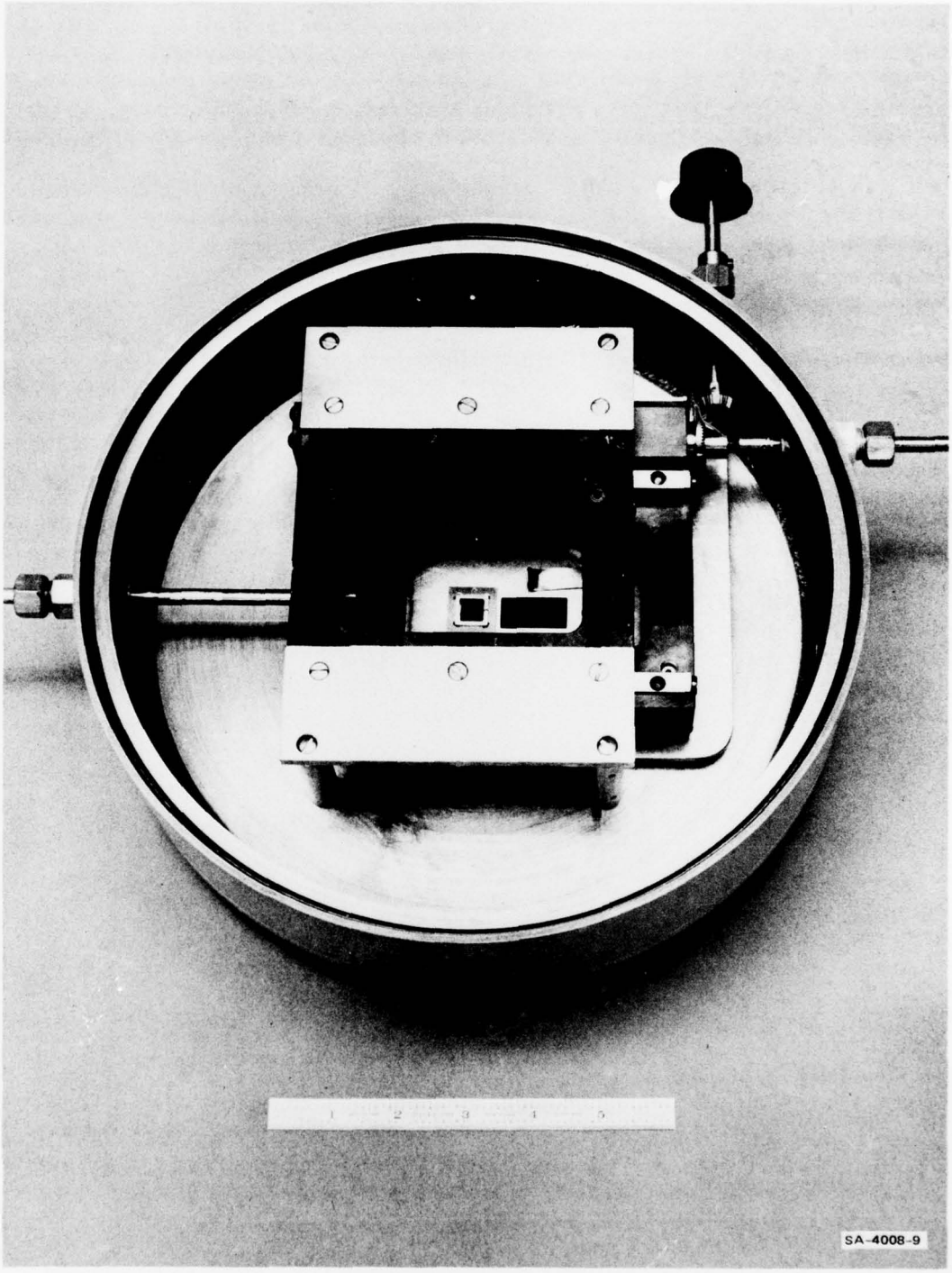

FIGURE 9 SAMPLE HOLDER

In addition to the sample holder, the stage incorporates a Faraday cup for measuring the total beam current and a transparent phosphor screen that can be viewed with a low-power microscope attached to the top of the EPES. The microscope allows the general detail of the pattern to be viewed for the initial setup. Phosphor resolution is sufficient to enable the operator to produce the most uniformly illuminated image, but it is not good enough to allow the proper focus to be determined. Focus can be determined only by trial-and-error exposure of a number of different samples.

The sample holder is mounted directly to the stage, but it is insulated from it for a potential difference of 7000 V. The exposure time is controlled by using the sample potential as an electronic shutter. The beam is cut off from the sample when its voltage is made about 15 V more negative than the cathode voltage (-500 V), and for exposure the sample voltage is abruptly changed to about -8.3 times the cathode voltage (~ +4150 V). This method of shuttering has the advantage that between exposures the electron beam is shut off only in the very short region between the projection lens and the sample (~ 0.5 inch) and remains stable in the rest of the column. This stability is important, because the energy of the beam before the final lens is only 500 eV and is easily deflected by charge that can build up on interior surfaces. Exposure times are typically of the order of 10 seconds but can be as short as 1 second.

Tests were made on the resolution of the EPES by using a fine mesh screen supported over a 0.055-inch-diameter hole as a transmission mask. The intermesh spacing of the screen (50.8 μm) was demagnified by 19.2× and projected onto a silicon wafer coated with PMMA. A typical pattern obtained after development is shown in Figure 10 where the distance between adjacent exposures is 2.6 μm. The resolution demonstrated by this method is about 0.5 μm and should be adequate for IO devices.

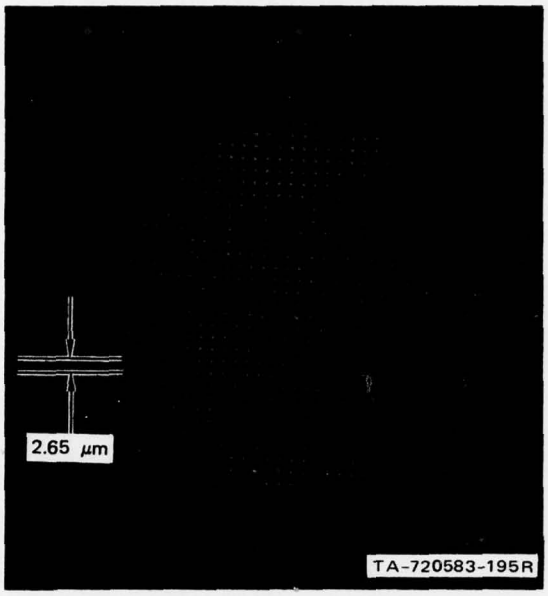

FIGURE 10 RESOLUTION OF A PROJECTION LENS

III FABRICATION OF ELECTRON TRANSMISSION MASKS

Fabrication of suitable electron transmission masks to form the uniform incident electron beam into the desired spatial pattern are essential for the successful production of the desired IO coupler pattern. Several conditions must be met for useful electron projection masks. Since the definition of the final coupler edge should be held to an acuity of 500 Å or better, a close tolerance (~ 1 μm at 20X reduction) is placed on the edge roughness permitted in the object mask pattern. Furthermore, the transmission masks must be made with effective support for the fine structure in the pattern. The pattern must withstand normal handling without developing defects; it must be sturdy enough that the pattern edges do not vibrate during exposure and destroy the edge resolution, and it must withstand the heating effect of the impinging electron beam.

We tried various methods of producing the high-resolution, structurally stable electron transmission mask needed for the EPES. The basis of these methods is the use of standard contact photolithography.

Because of the electron projection reduction of 20x, the use of photolithography is adequate to produce masks with the needed definition. The selective etching properties of silicon and metal films are used in the microfabrication process.

All the methods of making masks entail the use of silicon as a backing layer for a thin film of metallic gold in which the high-resolution pattern is etched. The silicon backing material is etched away preferentially to a slightly larger size than the pattern in the gold. This technique leaves the gold overhanging the edge of the silicon slightly to provide a high-definition pattern.

Basically, three techniques for the production of transmission masks were developed during this contract. The first technique consists of etching the silicon support with a nonselective plasma etch with SF_6 gas. A number of masks were made with the technique, but it was found very difficult to control the silicon etch rate uniformly over the sample, and frequently either the silicon support was removed completely or thin remnants of incompletely etched silicon remained behind in the transmission area. To increase the yield, a second technique using a selective etch process was tried. This method uses the orientation-dependent characteristics of silicon to certain aqueous etches, in particular to a 44% KOH solution heated to 85°C.[5] The selective etch enhances the depth to which the pattern can be etched into the top silicon surfaces without grossly undercutting the gold film as a nonselective etch would. The deeper pattern makes it easier to etch the wafer from the back without losing the silicon support. This technique was not entirely successful, because certain portions of the coupler pattern did not align exactly with the slow etching (111) planes of the silicon, and ragged edges resulted where the patterns tended to curve.

The third technique proved to be very successful, and substantially increased the ease of mask fabrication. This method relies on the fact that highly-doped silicon etches at a much slower rate than undoped silicon with certain etches.[5] Thus, if the silicon immediately adjacent to the gold layer is heavily doped, e.g., with boron, then, when the etch is applied to remove the silicon in the pattern areas, the etch will

slow down when it comes to within about 1 μm of the gold layer, because of the indiffused boron. This property makes it possible to obtain a final uniform thickness of silicon under the gold film to add to its mechanical support. Initial masks were produced with an aqueous silicon etch composed of ethylene diamine-pyrocatechol and water heated to 115°C in a reflex condenser. The fragility of such thinly etched masks made them difficult to handle in the hot aqueous etchant, and the aqueous technique was replaced by a gaseous etching technique using SF_6. This change of etchants increased the mask yield substantially, and subsequently all masks have been fabricated by SF_6 etch methods exclusively.

In detail the transmission masks are produced with the following sequence of steps.

1. A 2-inch-diameter wafer of [100] Si, 0.013 inch thick and polished on one side is washed in methanol, followed by ultrasonic agitation cleaning in isopropyl alcohol, rinsed in a flowing isopropyl alcohol solution and blown dry with a clean stream of warm, dry nitrogen.

2. A thin film of dopant solution is spun onto the clean wafer at a speed of 4500 rpm. The dopant we used is Emulsitone's Type-B Borofilm (Emulsitone Company, 19 Leslie Court, Whippany, NJ). This procedure produces dopant concentrations in excess of 2×10^{19} cm^{-3}.

3. The wafer is heated to 1150°C in a tube furnace for 1 hour in an argon atmosphere.

4. The diffusion of boron into the top surface of the wafer is completed with a 25.4-hour heating period at 1200°C. The final depth of diffusion is about 12 μm.

5. As a by-product of the last step, a heavy oxide film is formed on the wafer surface. This layer is removed in a solution of HF and H_2O (1:1) at room temperature.

6. The wafer is now diced into squares 0.75 inch on a side.

7. The dice are ultrasonically cleaned in isopropyl alcohol to remove the Si fragments created by the dicing operation and are then blown dry with warm nitrogen.

8. The surfaces are sputter cleaned in an RF sputter unit; a deposit of SiO_2 is then sputtered on, to a thickness of about 1500 Å.

9. A thin layer of chromium (1000 Å), followed by a 1.2 μm of gold, is next sputter deposited (approximately a 1-hour deposition at 300 V).

10. Shipley positive photoresist AZ-111 is spun onto the gold to a thickness of 6000 Å (3500 rpm spinner speed) and then baked at 70°C for 20 minutes.

11. The pattern is exposed in a mask aligner with an ultraviolet lamp. A typical exposure time is about 4 seconds.

12. Development is carried out in a 1:4 mixture of Shipley developer and H_2O for 30 seconds. The surface is dried in a nitrogen stream.

13. Post-baking is done in two steps: a drying operation at 70°C for 2 hours and a resist-hardening step at 170°C for 20 minutes.

14. The gold film unprotected by the resist is sputtered away. This process takes about 2 hours at 1000 W RF. During this etch some of the silicon dioxide is also removed.

15. The remaining oxide is etched with a standard buffered oxide etchant (BOE).

16. The boron-doped silicon in the pattern is then removed to a depth of 10 to 15 μm, with a mixture of HF and HNO_3 (3:7). An etching time of 20 to 30 seconds is generally sufficient.

17. To protect the pattern in subsequent processing, the etched channel is filled with a mixture of AZ-111 and monochlorobenzene (3:1). Care must be used in applying this mixture so that no air bubbles become trapped in the pattern.

18. The AZ-111 filler is dried at 70°C for several hours.

19. The silicon die is now inverted, and the area surrounding the pattern is masked with an alumina mask. Metal masks seem to affect the etch rate, and the result is a slower and less uniform etching. Areas not easily protected by the alumina mask can be coated with a layer of AZ-111, but this layer will probably need to be renewed several times during the plasma etching process. The plasma etching uses SF_6 gas at a pressure of 250 microns. The gaseous discharge is sustained with a voltage of 600 V rms and a power of 75 W. The etch rate decreases markedly when the undiffused boron layer is reached, and the etching can be observed directly to determine when the pattern is complete.

20. The AZ-111 filler is removed in acetone, followed by a flush with isopropyl alcohol and hot dry nitrogen.

21. As a final step, gold is deposited on the back side of the silicon die. This operation has two effects. It coats the back of the exposed SiO_2 with a conductive layer to reduce charging during use in the EPES. Furthermore, with no coating the tension of the gold on the front side of the mask tends to curl the thin supporting membrane; by coating gold on the reverse the tension is compensated and the mask curl is reduced.

IV DEVICE FABRICATION USING EPES

For the project we designed and fabricated two optical masks for transmission mask production. Figure 11 shows the two mask patterns used for initial mask fabrication tests. These two masks include one that produces a region of high coupling and one that produces a low coupling region. The masks are designed so that their images can be juxtapositioned with the EPES rotary mask holder and sample stage.

The high coupling region is sandwiched between two low coupling regions that serve as inputs and outputs. Approximate theories [6,7] were

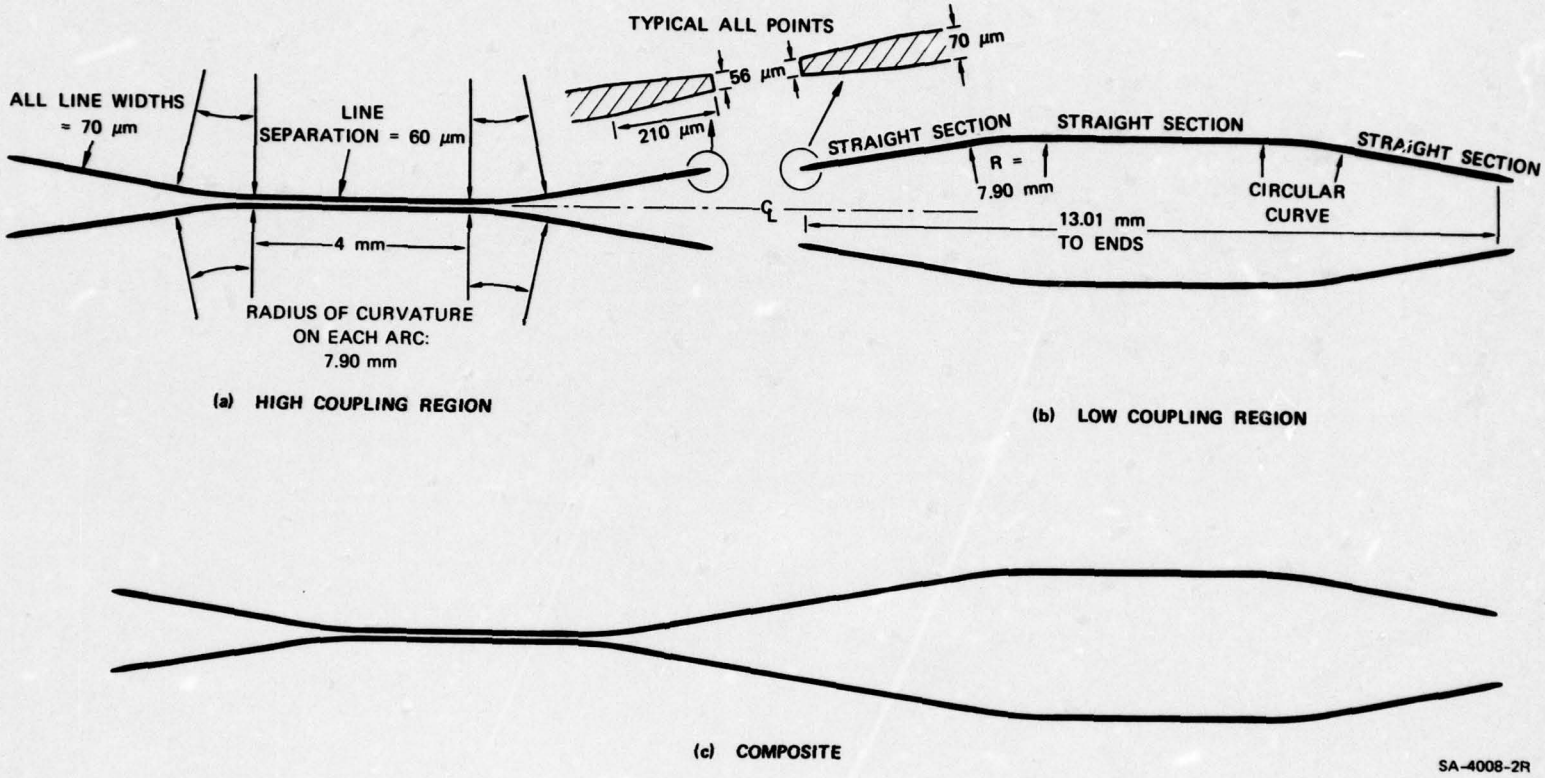

FIGURE 11 OBJECT MASK PATTERNS FOR IO COUPLER

used to establish the critical dimensions of the simple mode waveguides and coupler region.

When the patterns are reduced twenty times by electron projection, the 70 μm wide line should produce a single-mode guide in the diffused lithium niobate ($\Delta n \sim 0.01$). The line separation (in the high coupling region) was calculated to give about 3-dB coupling over the close proximity region. The smooth areas of the separation region were designed to yield low loss[8] (< 1 dB) and are tapered at 10 degrees to the axis. In the overlap region, where the two patterns are to be joined, the line width narrows by 20%. This arrangement compensates for any line broadening effect of having two electron-beam exposures in this region. The low coupling region was designed to provide:

- Nearly zero power exchange between guides
- A region where phase-shift electrodes can be formed if a switch is to be made.

The optical masks, obtained from Bell Industries (Photomask Division, 1165 Fairoaks Ave., Sunnyvale, CA), were of reasonably good quality. However, they suffered small systematic faults that may be attributed to the manner in which the computer-generated patterns were composed. Specifically, the discrete digital motion of the light exposure apparatus produces small steps along regions that should have continuous arcs. This may be a problem for the highest-quality IO patterns and would be difficult to eliminate because the digital stepping is inherent in the photomask production technique.

Several transmission masks were fabricated in gold on silicon by using the process discussed in the last section. Both sections of the IO patterns were fabricated. Figure 12 shows the etching of the coupler legs on a mask of the high coupling region. Good definition of the waveguide regions was obtained with the mask fabrication procedure. In general, the edge smoothness of the transmission masks was less than 1 μm, giving a theoretical edge roughness in the final pattern (after 20× reduction) of less than 500 Å.

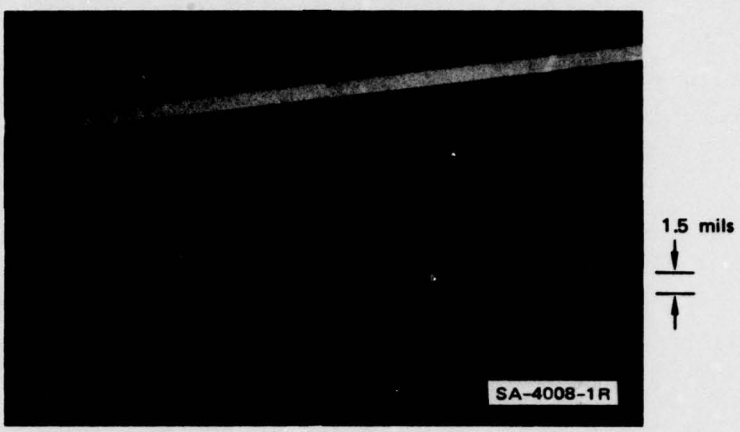

FIGURE 12 TRANSMISSION MICROGRAPH OF OBJECT MASK PATTERN

The low coupling pattern was the easier to fabricate because there was ample material for support between the long cut-out waveguide sections. However, the high coupling region presented some extra fabrication problems, because the long support distance (4 mm) between the two waveguides is only 60 μm wide. A mask was successfully fabricated with the technique, but, in general, masks of this design are too fragile to be practical. To overcome the breakage problem, the mask was redesigned to have only one leg of the coupler (i.e., imagine the pattern in Figure 11 bisected between the two waveguides). This design completely eliminates the fragility problem because all portions of the mask are strongly supported. Two identical waveguides of this type are fabricated and then positioned in the rotary mask holder so that by exposing each mask in sequence, the entire high coupling region is imaged onto the sample. Dividing the high coupling region between two masks has the added advantage that the coupling distance between the two waveguides can be adjusted when the masks are lined up under the toolmaker's microscope. Thus it is possible to change the coupling distance without having to produce a new photomask and then fabricate a different transmission mask. Several of these split high coupling region masks were produced for use in the EPES.

During the past year substantial improvements in the electron optical column, and its convenience of use were made. Three different lens configurations were tried and line widths of better than 0.5 μm were obtained. However, the key problem of uniformly illuminating the area of the transmission mask with electrons was not solved, and the final alignment tests for juxtapositioning the electron optical patterns for sequential exposures could not be made. For these reasons it was not possible to produce actual devices in the EPES system during the term of the contract.

V DEVICE FABRICATION USING OPTICAL CONTACT LITHOGRAPHY

Using the Qualitron masks and lithium niobate substrates supplied by NRL, we made four attempts to make devices using optical lithographic techniques according to the following procedures:

1. The polished surface is cleaned with acetone, alcohol, Transene-100 (Transene Co., Inc., Rowley, MA) and blown dry with dry N_2.
2. Shipley AZ-1350 positive photoresist is spun onto the polished surface of the crystal at 4000 RPM.
3. Resist is prebaked for 30 minutes at 75°C.
4. The optical channels are delineated using mask QM-31015 with a 12-second exposure under mercury vapor lamp. The resist is developed in Shipley AZ developer for 90 seconds and rinsed thoroughly in water. The resist is allowed to dry overnight without a postbake.
5. The surface is sputter cleaned in an oxygen glow discharge for 3 minutes.
6. The sample is rapidly transferred to a vacuum system and pumped to 10^{-6} torr. Titanium is evaporated by an electron beam at 1.5 to 2.0 Å/minute to a thickness of 175 Å. The rate and total thickness are monitored with a Inficom XTM quartz crystal monitor.

7. The resist and its coating of titanium are lifted in acetone with a very gentle ultrasonic agitation. (Note: if the ultrasonic bath is warm due to prior operation, and/or agitation is violent, the crystal may fracture. Successful lift off was obtained with a Dynasonic Model G-6 135W ultrasonic unit on the lowest power setting.)

8. The titanium is indiffused in argon at 1000°C for 5 hours. A rise time of 2.5 hours is used. The argon is shut off after cooling to 950°C and oxygen is admitted for the remainder of the controlled cool down to 600°C in 2 hours. The crystal is removed when the furnace has reached room temperature. This oxidation insures niobate stoichiometry.

9. After a thorough cleaning, a chromium film of 200 Å is deposited on the surface, followed by 2000 Å of gold.

10. Shipley AZ-1350 positive photoresist is spun on at 4000 RPM.

11. The resist is baked for 30 minutes at 75°C.

12. The metal electrode pattern is exposed using mask QM-31016 and a 12-second exposure to mercury vapor lamp. [Note: The mask alignment step is most critical. Not only is the pattern of the optical channels very difficult to see through the gold film as slight surface irregularity in the underlying surface, but the dimensions of the crystal (25 mm X 6 mm X 3.5 mm) and the glass supported photomask are not compatible with conventional mask aligner design. The pattern must be positioned to micron dimensions, and position adjustments are very difficult to accomplish without damaging the gold deposit.]

13. The resist is developed with Shipley AZ developer and post-baked 60 minutes at 100°C.

14. The gold is removed in the open areas using a sputter etch procedure.

15. The resist covering the electrode pattern is removed with Shipley 1112 remover, leaving the electrode pattern.

16. Gold leads of 1.5-inch length are bonded to the contact pads.

The first set of devices successfully passed waveguide fabrication, and two parts with eight pairs of optical channels apiece were shipped in October 1976. These did not have the gold phase shifting electrodes and were to be used by NRL to test the optical properties of the indiffused optical waveguides.

A second set of devices were fabricated but were rendered unusable when the lithium niobate substrates developed surface fractures during the ultrasonic cleaning step (Step 9).

The third set of devices successfully passed all their process steps but during the optical alignment became scratched to the point of being unfit for final testing (Step 12).

A fourth set of devices was attempted but in the titanium indiffusion step (Step 8), a cloudiness developed on the lithium niobate surface probably due to furnace contamination. Since this effect would render the devices useless, the fabrication attempt was abandoned at this point.

VI ACKNOWLEDGMENTS

The Principal Investigator and originator of much of the work reported here was E. R. Westerberg who terminated at SRI in February 1977 before completion of the project. The electron optical studies were picked up by Dr. T. E. Thompson, and Mr. J. B. Mooney carried out the photolithographic fabrication of the devices, both at very short notice. The project has benefitted from the outstanding skills of the technicians involved, namely G. Reich and J. Hunt. This final report was prepared by the project supervisor Dr. I. Brodie, drawing heavily on material previously prepared by Mr. Westerberg.

REFERENCES

1. L. I. Maissel, and R. Glang, eds., Handbook of Thin Film Technology pp. 7-18 (McGraw-Hill, New York, New York, 1970).

2. H. I. Smith, F. J. Bachner, and N. Efremow, "A High Yield Photolithographic Technique for Surface Wave Devices," J. Electrochem. Soc., Vol. 118, pp. 821-825 (May 1971).

3. D. L. Spears, and H. I. Smith, "High Resolution Pattern Replication Using Soft X-rays," Electronic Letters, Vol. 8, No. 4, pp. 102-104 (February 1972).

4. T. W. O'Keefe, "Fabrication of Integrated Circuits Using the Electron Image Projection Systems (ELIPS)," IEEE Trans. Electron Devices, Vol. ED-17, No. 6, pp. 465-469 (June 1970).

5. D. L. Kendall, "On Etching Very Narrow Grooves in Silicon," Appl. Phys. Letters, Vol. 26, No. 4, pp. 195-198 (15 February 1975).

6. E. A. J. Marcatili, "Dielectric Rectangular Waveguides and Directional Couplers for Integrated Optics," BSTJ, Vol. 48, pp. 2071-2102 (September 1969).

7. M. K. Barnoski, "Introduction to Integrated Optics," (Plenum Press, New York, New York, 1974), Chapter 6.

8. H. F. Taylor, "Power Loss at Direction Changes in Dielectric Waveguides," Appl. Optics, Vol. 13, p. 642 (March 1974).